Jurnal Fisika Flux: Jurnal Ilmiah Fisika FMIPA Universitas Lambung Mangkurat
Volume 18, Nomor 1, Februari 2021
1819-796X (p-ISSN); 2541-1713 (e-ISSN)

Heat Flow Transport Model by Gauss-Seidel Type Iteration Methods for Gas and Solid Materials

Nurlaela Rauf*), Heryanto Heryanto, Roni Rahmat, Dahlang Tahir
Department of physics, Hasanuddin University, Makassar, 90245 Indonesia

*n-rauf@fmipa.unhas.ac.id, Telp/Fax: (+62) 411-587634

DOI: https://doi.org/10.20527/flux.v18i1.8386
Submitted: 11 February 2021; Accepted: 15 March 2021

ABSTRACT- Technological processes for modification of materials, deposition, and prevented fumes in the pyrolysis processes are used gases materials in the medium with vacuum pressure or atmospheric air pressure. Therefore, it is essential to understand heat flow transport for designing an efficient reactor or find the substrate's excellent position in the reactor or furnace for growing materials. We evaluated the energy transfer phenomena in the form of temperature distribution and heat flow for various heating sources for the gases and solid materials by Gauss-Seidel equation. The thermal conductivity coefficient (k), number of heating sources, and position of heating sources show an essential parameter for transmitting the distribution of the heat. For high k value shows efficiently for heat transfer at low temperature due to the atom's position close each other. The heat also affects to the phonon and lattice vibration like a wave which successfully shows these phenomena in this study.

***KEYWORDS*:** Gauss-Seidel; Gas and Solid Materials; Heat flow; Heat penetration; Thermal conductivity coefficient

INTRODUCTION

Technological processes usually used gases materials for modification of materials by using plasma/beam with and without hotwire, dry deposition of silicon dioxide on silicon wafer in the furnace, and for prevented fumes in the pyrolysis processes (Vitanov, Harizanova, Ivanova, & Dikov, 2014; Tianbai, Kun, Qingdong, & Tiezheng, 2018; Michael & Alexandre, 2020). For creating plasma/beam with or without hotwire, usually in the medium with vacuum pressure but for furnace and pyrolysis in the medium without vacuum pressure or atmospheric pressure air.

For atmospheric pressure air are intensively developed for applications plasma-assisted combustion, and pollution control by generation of reactive species in chemical reaction (Aoife & Jerry, 2019; Hammer, 2014). Therefore, it is essential to understand the heat flow transport for designing an efficient reactor or find very good position of the substrate in the reactor for growing materials or to find maximum position flow of the gases in the furnace. Gas flow as the effect of temperature is one of the essential discharge parameters because gas temperature affects the chemical reactions and densities of gases, leading to different discharge chemistry. The gas flow and temperature also influences to the transport properties of species, which may result in different transport behavior. Hence, it is important to analyze the heat flow of gases and some solid materials for different positions of heating sources to find maximum chemical reaction for modification materials or deposition or prevented fumes in the pyrolysis processes. For these purposes, in this study, we have evaluated the energy transfer phenomena in the form of temperature distribution and heat flow in two and three dimensional and various heating sources for the gases and solid materials by

mathematical equations which completely solved with numerically simulation (Da Silva, Prado, & Fernandes 2017; Farahani, Yerra, & Pilla, 2020; Gregori *et al.*, 2020).

Heat transfer is one of the physical phenomena which described the Laplace or Poisson partial differential equation (Mortazavi & Moghaddam, 2016; Idesman & Dey, 2020; Conte, 2020; Berezansky & Braverman, 2020). Heat transfer is a concept for predicting energy transfer due to the temperature differences between two positions or materials, which can be observed by the direction of moving particles or by the effects (Liu, Wang, & Yi, 2020; Karami & Kamkari, 2020; Zhang, Gao, & Huang, 2017).

The possibility to get maximum energy savings is by reducing the heat flow[16] for analysis of the different thermal properties of each material (Wu *et al.*, 2020; Shen & Zhou, 2020; Al Amin *et al.*, 2018). Heat flow rates of various materials are presenting in the form of differential equations which can be solved by numerical methods if analytic methods are rated difficult (Boland, 2002). Numerical methods to solve partial differential equations usually utilized the Crank-Nicolson, Milne, Hamming, and Gauss-Seidel method (Akgül & Modanli, 2019; Gao, 2016; Zhang, Gao, & Huang, 2017; Wu, Zhou, & Chen, 2020). Gauss-Seidel equation is recurring calculation that can solve algebraically on unknown variables for linear or nonlinear algebra which suitable for energy transfer problems.

In this work, we have applied the Gauss-Seidel equation as an energy transfer solution in the iteration methods for the matrix models of heat flow. Several heating sources are varied from one side, from the corner of two and three dimensional, from two sides, and four sides of the wall. The models of temperature distribution and the flow of the heat will be chosen as the final result of these energy transfer phenomena in gas and solid materials.

SCHEME AND PARAMETER

The Gauss-Seidel method is a partial solution from the differential equation obtained for the schematic model in Figure 1. The temperature distribution was carried out based on a schematic model with an adjustable heat source position to apply this method. In the first scheme (left), We have used three schemes based on dimensional of insulating wall in this study. The first scheme is two heating sources, the second scheme is four heating sources and in the third scheme, there are formed a three-dimensional building with four heating sources (see Figure 1).

Figure 1 represents three schematic models in this study, the temperature for space with T_1 is 270 K, and the other surface with T_2 is 298 K. The sheeting materials (k_s) are for glass, which wrap material for the phase of gas.

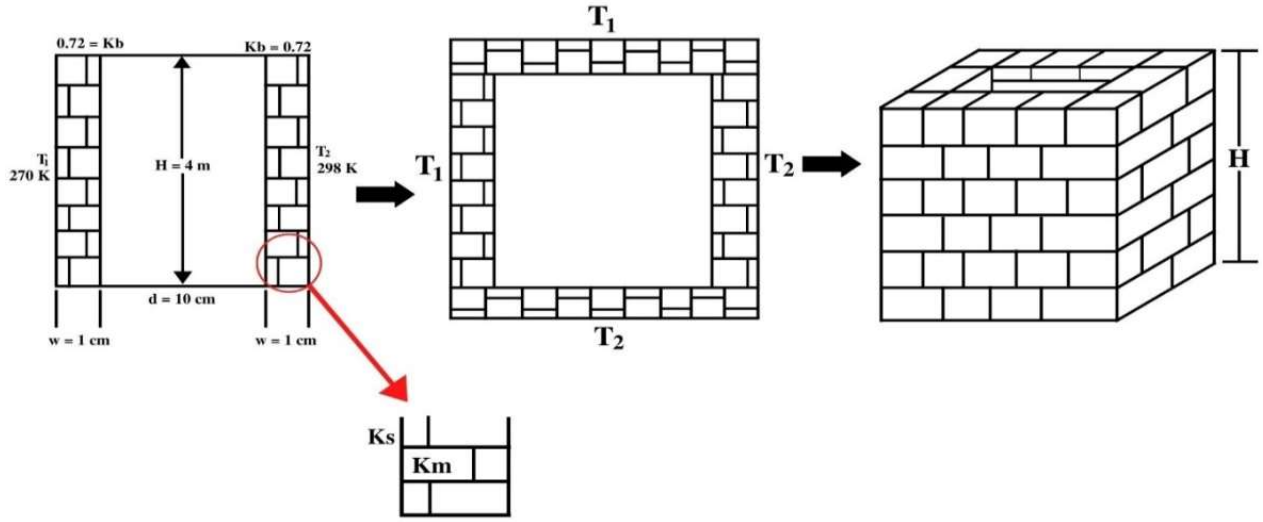

Figure 1 Schematic illustration model for the insulating wall: two sides of a two-dimensional wall (left), four sides of a two-dimensional wall (middle), and the three-dimension of wall (right).

Parameters:

k is thermal conductivity coefficient ($Wm^{-1}K^{-1}$) (www.EnggineeringToolBox.com (1), 2020; www.EnggineeringToolBox.com (2), 2020):

k_B : 0.72 (Brick) k_A : 0.05 (Air)
k_{CO} : 0.0231 (CO) k_{CO_2} : 0.0146 (CO_2)
k_{Glass} : 1.05 (Glass) k_{H_2S} : 0.013 (H_2S)
k_H : 0.168 (H)

k is thermal diffusivity coefficient (m^2s^{-1}) (Brun and Pacheco, 2005):

k_A : 1.45×10^{-5} (Air)

Another variable

σ : Stefan-Boltzmann constant 5.67051×10^{-8} $Wm^{-2}K^{-4}$
Nu : Nusselt number

Emissivity of a surface (ε) (Brun and Pacheco, 2005):

ε_B : 0.9 (brick)

ρ (Densities) in unit (kg/m^3)

The $T_0 = T_2 - T_1$ for heat flow for conduction (q_{cond}) substitute to the equation (5) and resulting equation (9) (Brun & Pacheco, 2005):

$$k(\Delta y * 1)\frac{A_{21} - A_{22}}{\Delta x} + k(\Delta x * 1)\frac{A_{32} - A_{22}}{\Delta y} = k(\Delta y * 1)\frac{A_{32} - A_{23}}{\Delta x} + k(\Delta x * 1)\frac{A_{22} - A_{12}}{\Delta y} \quad (1)$$

(Δy * 1) and (Δx * 1) are heat transfer areas, multiplying with 1 because of their interior nodes. The (*1) considered as the two-dimensional grid, and by applying the Fourier's law, the equation (1) become:

www.EnggineeringToolBox.com (2), 2020):

ρAir : 1.225 ρCO : 1.14
ρH : 0.089 ρH_2S : 1.36
ρCO_2 :1.98 ρBrick : 2400
ρGlass : 2500

NUMERICAL TECHNIQUES

Temperature distribution

The previously stated that, the numerical method by the Gauss-Seidel equation is recurring calculation that can solve algebraically on unknown variables. It can solve a set of linear or nonlinear algebra which suitable for energy transfer problems (Pu & Yuan, 2019; Klametsdal, Rasmussen, Meyner, & Lie, 2020; He & Wang, 2019; Paradezhenko, Melnikov, & Reser, 2019). The grid of the column's sectional area for Gauss-Seidel calculation is shown in Figure 2.

$$\frac{A_{23} - 2A_{22} + A_{21}}{\Delta x^2} = -\frac{A_{12} - 2A_{22} + A_{32}}{\Delta y^2} \quad (2)$$

For the $\Delta x = \Delta y = \Delta xy$, the equation (2) becomes:

$$\frac{A_{23} - 2A_{22} + A_{21}}{\Delta xy^2} + \frac{A_{12} - 2A_{22} + A_{32}}{\Delta xy^2} = 0 \quad (3)$$

multiply with Δxy^2

$$A_{22} = \left(\frac{A_{12} + A_{21} + A_{32} + A_{23}}{4}\right) \quad (4)$$

The temperature distribution must be repeated in the processes using the equation (4) to find a suitable matrix. The first step is determining the size of the matrix with a high correlation with the number of iterations, consequently controlling Δx and Δy. The

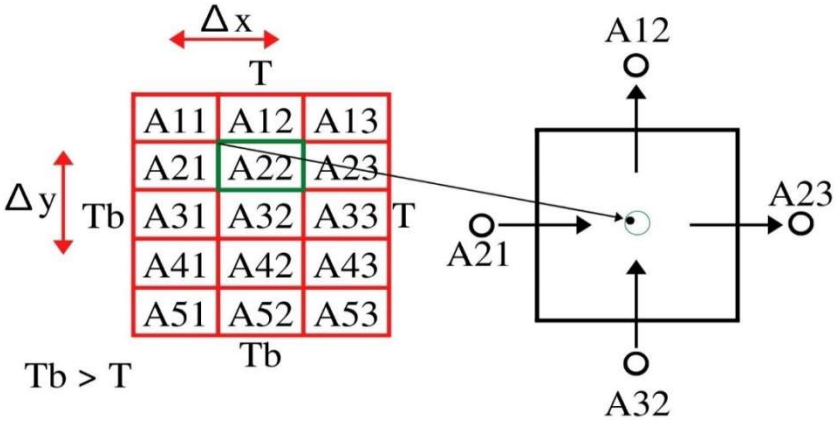

Figure 2 The illustration schema of grid model for Gauss Seidel method for determining the matrix value where the first number of grid model indicated row and the second number is column of the matrix.

second step is to determine the amount of energy applied in this case; there are four heating sources positions: up, down, left, and right. The heating source position difference will give a different contour or model of energy distribution in the material. The third step is preparing an iteration boundary, where the process follows equation (4). According to scheme two (middle), heat will continue from the four different positions of the same conditions applied for other materials. In this case, we focus on determining heat flow characteristics through the wall, as shown in Figure 1 for the scheme and the various solid and gas materials.

Heat flow

In general, heat is transmitted by conduction, convection, and radiation. The simple way to write for all three types of heat flow can be written as follows (Brun & Pacheco, 2005):

$$q_{cond} = \frac{k}{d}\left(T^{"} - T'\right) \quad (5)$$

$$q_{conv} = h(T^{"} - T') \quad (6)$$

$$q_{rad} = \frac{\varepsilon}{2-\varepsilon}\sigma\left(T^{"4} - T'^{4}\right) \quad (7)$$

Heat flow for conduction (q_{cond}) as shown in equation (5) by entering equation $T_0 = T_2 - T_1$ (Brun & Pacheco, 2005), where we can apply on the figure 1 for the first scheme, it will be obtained:

$$T'' = \frac{k_m T_2 d + 2wkT_0}{k_m d + 2wk} \quad (8)$$

$$q_{cond} = \frac{k_m}{w}(T_2 - T'') \quad (9)$$

By substitution the T'' (eq. (8)) into the equation (9), the results is q_{cond} as follows:

$$q_{cond} = \frac{2k_m k(T_2 - T_0)}{(k_m d + 2wk)} \quad (10)$$

Heat flow for convection (q_{conv}) as shown in equation (6) with assumption that the air is filling the wall, the q_{conv} can be written as (Brun & Pacheco, 2005):

$$q_{conv} = \frac{k_m \Delta}{2w}\left(\frac{f}{1+f}\right) \quad (11)$$

Where $f = \frac{2wk_a Nu}{k_m d}$ is (0.790ln(Re) - 1.64)-2 , 104 < Re < 106 Nusselt number (Nu) for smooth tubes and the $Nu = \frac{hd}{k}$, k_m is coefficient of thermal conductivity of materials, w is width, h is height of the wall, and d is the distance between the wall.

Heat flow for radiation (q_{rad}) as shown in equation (7) which follow the scheme 1 in Figure 1 (left) shows radiation from T_2 to T_1 (Brun & Pacheco, 2005):

$$q_{rad} = 4\frac{\varepsilon}{2-\varepsilon}\sigma\left(\frac{T_0^3(T_2 - T_1)}{1 + 8cT_0^3}\right) \quad (12)$$

Brun and Pacheco (2005) reported $c = \frac{w}{k_m}\left(\frac{\sigma\varepsilon}{2-\varepsilon}\right)$, which use to determine the relationship between the width of the material and the radiation heat flow, as described in equation (12). The duration of the penetration heat for any kinds of materials with stationary conditions as follows for three dimensional:

$$\rho c_p \frac{\partial T}{\partial t} = k_m\left(\frac{\partial^2 T}{\partial x^2} + \frac{\partial^2 T}{\partial y^2} + \frac{\partial^2 T}{\partial z^2}\right) \quad (13)$$

Where T is describe the diagonal distribution temperature.

RESULT AND DISCUSSION

The heating process by convection q_{conv} shows higher value followed by conduction q_{cond}, and q_{rad} processes, it is shown the best agreement with Brun and Pacheco (2005). The atoms give out heat as a phonon for the heating process and produce lattice vibration, which may be like a wave. The wave motion will transport the amount of energy that strongly depends on the distance from the sources; consequently, it will give the convection and conduction's different value.

Figure 3 shows the heating process for conduction (a) and convection (b) as a function of the distance from the sources, which depend on the type of materials; the thermal conductivity coefficient, and the corresponding result is presented in Table 1. The high value of conduction from the gas materials, whereas metal material shows the low value of conduction may due to the distance between the atomic is close to each other (Lu *et al.*, 2020). The equation (10 and 11) clearly shows that the high thermal conductivity coefficient values will produce high heat flow for conduction and for convection process (Luijendijk, 2019). The convection process strongly depends on the

convection coefficient (*h*), as shown in equation 6, which may due to the molecular properties of materials (Defraeye, Blockenc, & Carmeliet, 2013).

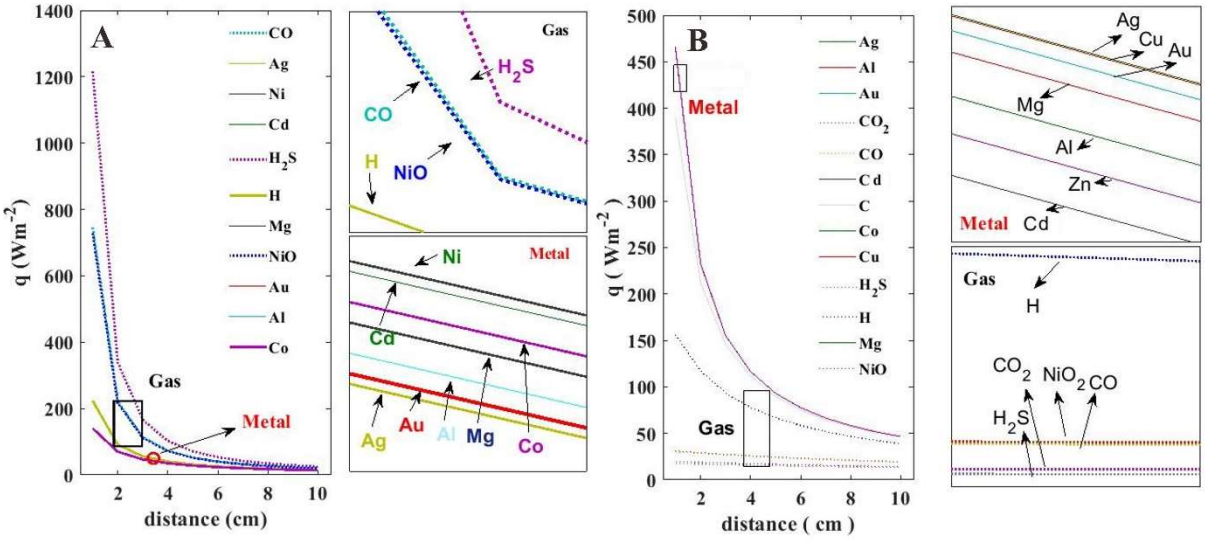

Figure 3 Heat flow for conduction process ($q_{cond.}$) (a) for convection process ($q_{conv.}$) (b), for several types of material and gas.

Table 1 The relationship between the distance and the heat flow for the three different heat processes: by the conduction ($q_{cond.}$), the convection ($q_{conv.}$), and the radiation ($q_{rad.}$) for the distance 1 cm to 10 cm from the heating source.

d (cm)	1	2	3	4	5	6	7	8	9	10
q_{cond} (Wm^{-2})	159.44	74.86	48.82	36.21	28.77	23.87	20.3	17.8	15.7	14.19
d (cm)	1	2	3	4	5	6	7	8	9	10
q_{conv} (Wm^{-2})	318.64	189.23	134.57	104.41	85.30	72.10	62.44	55.06	49.24	44.53

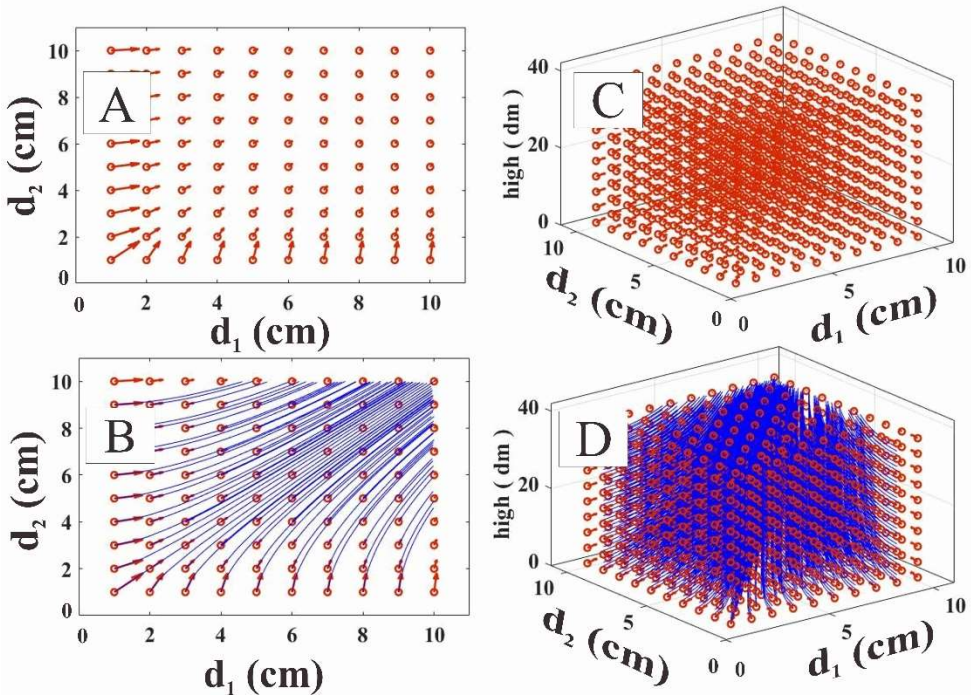

Figure 4 Heat flow diagram for 2 dimensional (up) (a) for without streamline and (b) for with streamline and 3 dimensional (bottom) (c) for without streamline and (d) with streamline.

Figure 4 shows the heat flow diagram from the corner position (0,0) for two dimensional and three dimensional without streamline (left) and with streamline (right) by the conduction process. The heat flow from the corner position to the diagonal of another corner position indicated that all atoms in the material would bring the energy from one atom to the next atoms (Motlagh & Kalteh, 2020). It is looks–like the relay runner.

Figure 5 shows the heat temperature distribution, d is 10 cm with minimum T is 270^{o}K, and the maximum temperature is T_2 at the boundary based on scheme 2. The more solid image can be obtained by the Gauss-Seidel approach that allowed the user to create a large matrix and modify the computational method's heat source position (Basuki, Cari, & Suparmi, 2017). Modifying the heat source position will have provided information for the heat transfer conditions to find the homogenous distribution of temperature for the best correlation with the experimental conditions.

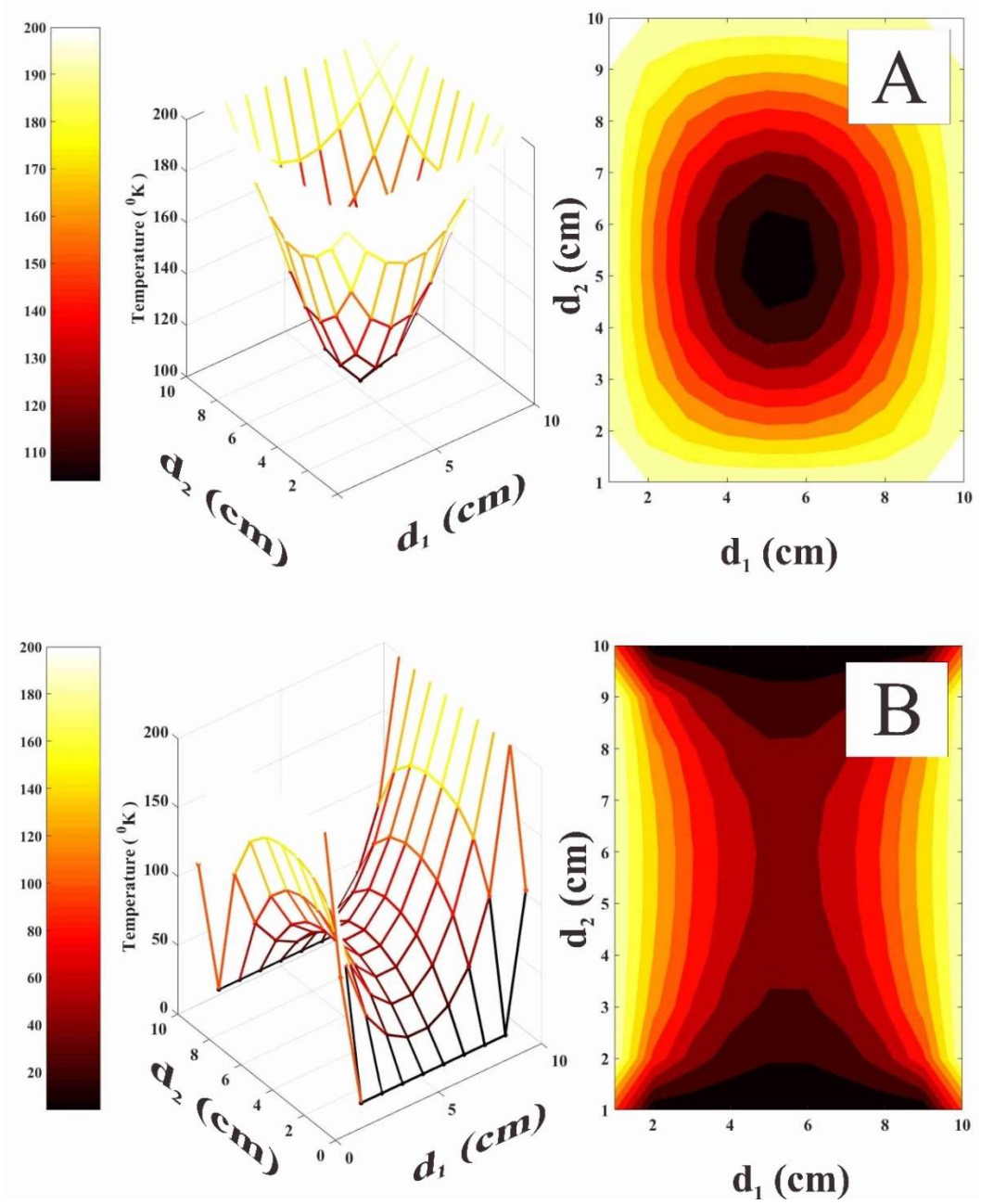

Figure 5 Temperature distribution by Gauss-Seidel methods: right for two dimensional and left for three dimensional, for (a) 4 sources based on the scheme 2 in Figure 1 (middle) and (b) 2 sources based on the scheme 1 in Figure 1 (left).

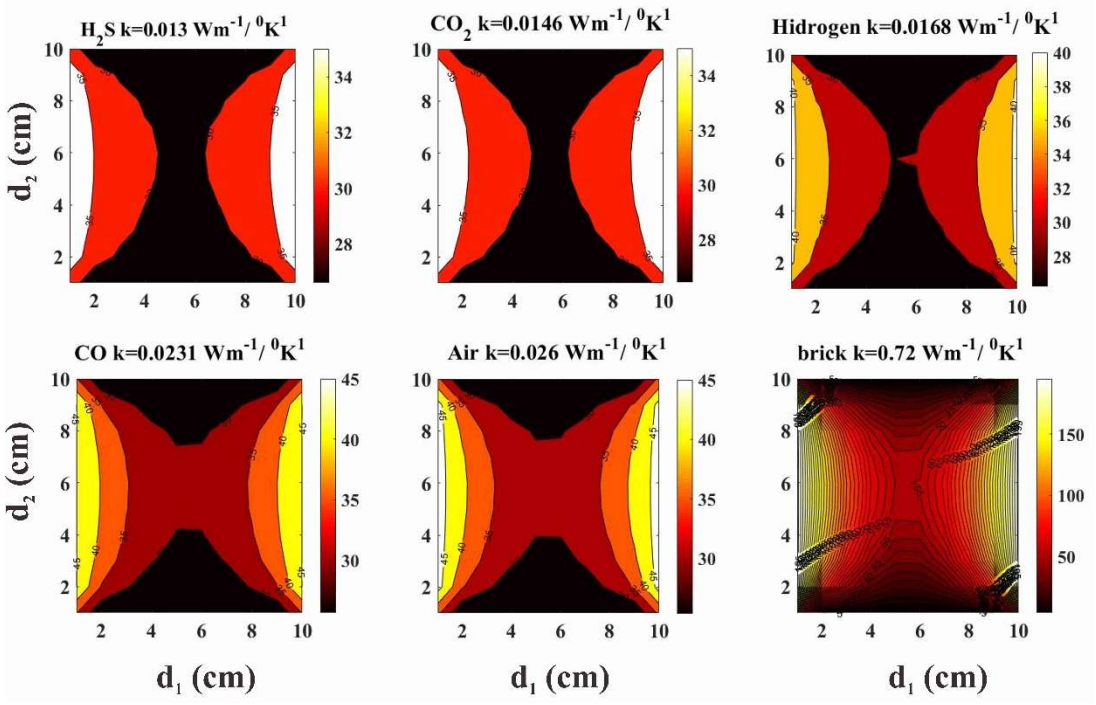

Figure 6 the contour of temperature distribution for the different type of materials with two heating sources in left and right side (from the left to the right, first rows: H_2S, CO_2, H, second rows: CO, Air, Brick)

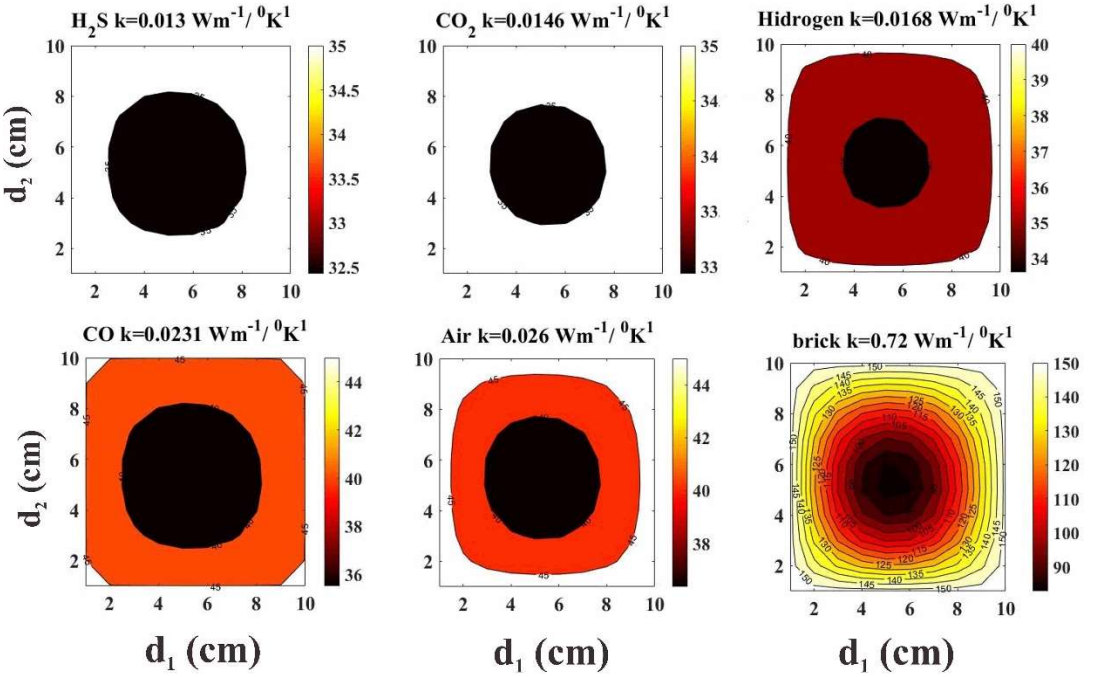

Figure 7 The thermal distribution (contour) for four side of heating sources show strongly dependent of the thermal conductivity coefficient of the materials for low (left) to the high (right) and also included the brick materials for comparison.

Temperature distribution for scheme 1 in Figure 1 (left) by using:

$$\rho c_p \frac{\partial T}{\partial t} = k_m \left(\frac{\partial^2 T}{\partial x^2} + \frac{\partial^2 T}{\partial y^2} + \frac{\partial^2 T}{\partial z^2} \right) \qquad (14)$$

The equation (14) determined and classified of temperature distribution for several types of gas materials with specific values of k_m and k_s. Figure 6 shows the surface contour of the temperature distribution by two dimensional for several types of materials.

Figure 6 shows contour level of heat distribution at low k-value for gas material and solid materials (brick) for two sides of heating sources (left and right) and for Figure 7, four

heating sources (left, right, bottom, top). The sheeting materials are glass ($k_s \approx 1$), where the width is $wk_s \approx 0.1$cm << d, and used to keep the material from evaporating at the barrier wall for the gas material. The contour of temperature distribution is affected by the thermal conductivity coefficient, the number of heating sources, and the position of heating sources ex. for four different sources based on scheme 2 in Figure 1(middle) (Dogu & Aksit, 2006).

Figure 7 shows the thermal distribution for gas material and brick by four sides of heating sources. The thermal conductivity coefficient (k) shows an essential parameter for transmitting distribution, the number and position of heating sources also high effect to the contour of thermal distribution. For a material that has a high *k* value, has the high ability to transmit the heat, even at low temperatures, as clearly shown in the contour thermal distribution in Figure 7. This phenomenon is useful for identification of thermal penetration process in any materials. The relationship between thermal reductions is proportional inversely to the thermal penetration, as clearly shows in Figure 8 for various types of materials. The penetration of thermal can be described by temperature function based on the equation (14) with the analytical solutions, clearly seen in Figure 8 and corresponding results presented in Table 2.

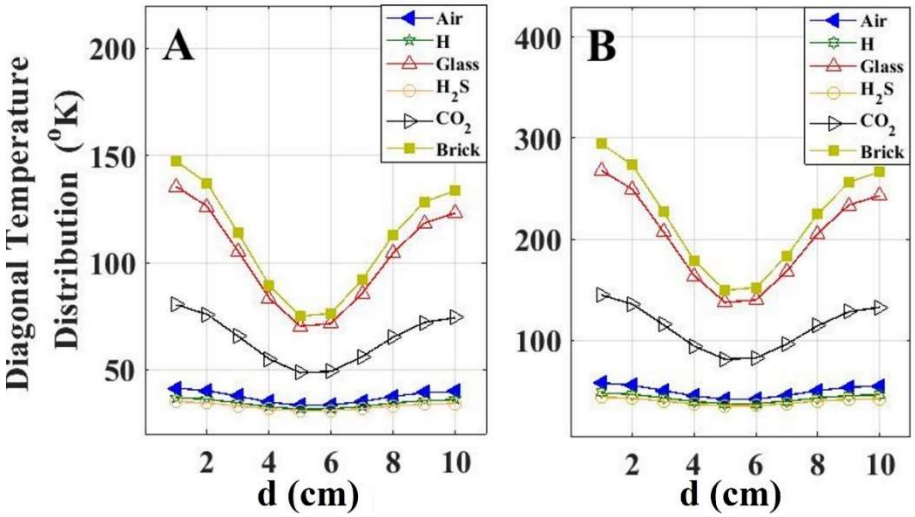

Figure 8 Temperature penetration for various materials as a function of distribution temperature and distance from heating (a) for 2 sources and (b) for 4 sources

Table 2 The analytical solutions of equation (14) from the analysis of Figure 8 from 2 and 4 heating sources with the distance between two wall materials are d1 is for 1 cm and d10 for10 cm

Materials	$\frac{k_m}{\rho c_p}\left(\frac{\partial^2 T}{\partial x^2}\right)$ 2 S	$\frac{k_m}{\rho c_p}\left(\frac{\partial^2 T}{\partial x^2}\right)$ 4 S	Heat penetration (°K/t) 2 S d1	2 S d10	4 S d1	4 S d 10
H	$\frac{k_H}{\rho c_p}(-0.045 * d + 0.72)$	$\frac{k_m}{\rho c_p}(-0.09 * d + 1.46)$	0.088	0.041	0.18	0.073
CO	$\frac{k_{CO}}{\rho c_p}(-0.006 * d + 0.98)$	$\frac{k_{CO}}{\rho c_p}(-0.12 * d + 1.8)$	0.019	0.018	0.032	0.011
CO_2	$\frac{k_{CO2}}{\rho c_p}(-0.264 * d + 4.2)$	$\frac{k_{CO2}}{\rho c_p}(-0.52 * d + 8.4)$	0.034	0.015	1.28	1.27
H_2S	$\frac{k_{H2S}}{\rho c_p}(-0.0354 * d + 0.58)$	$\frac{k_{H2S}}{\rho c_p}(-0.072 * d + 1.14)$	0.021	0.01	1.137	1.111
Air	$\frac{k_{Air}}{\rho c_p}(-0.066 * d + 1.08)$	$\frac{k_{Air}}{\rho c_p}(-0.132 * d + 2.2)$	0.021	0.01	2.197	2.172
Brick	$\frac{k_{Brick}}{\rho c_p}(-0.6 * d + 9.6)$	$\frac{k_{Brick}}{\rho c_p}(-1.2 * d + 19.4)$	0.002	0.001	0.005	0.002

Heat penetration according to Table 2, shows which directly proportional to (k) coefficient of thermal conductivity and inversely proportional with specific heat in a constant pressure process (c_P) and densities (ϱ) as the effect of damped wave transport and relaxation at the lattice of the molecule (Stanley, 2019).

FINAL COMMENT AND RECOMMENDATIONS

There has been a significant difference in the heat transfer process by gas and solid materials for transferring the energy. The value of k, cp, and ϱ depends on the type of materials, position, and number of heating sources that significantly affect temperature distribution, heat flow, and heat penetration. We apply Gauss-Seidel methods for simulation of the energy transfer for gas material (H_2S, CO, CO_2, H, and Air) and solid material (glass and brick) which more easily applied in the simulation for any types of materials. The position and quantity of the heating sources in determining the thermal distribution and the propagation of energy still needs further study. The improvements of the modeling for the complex conditions are needed and compared with experimental data.

ACKNOWLEDGMENTS

This work was supported by the PD (Penelitian Dasar) funded by the Indonesia Government (Kemenristek/BRIN) grants: 1516/UN4.22/PT.01.03/2020.

REFERENCES

Al Amin, A., Sabri, L., Poole, C., Baig, T., Deissler, R.J., Rindfleisch, & Martens, M. (2018). Computational homogenization of the elastic and thermal properties of superconducting composite MgB_2 wire. *Composite Structures*, *188*, 313-329. https://doi.org/10.1016/j.compstruct.2017.12.060

Akgül, A., & Modanli, M. (2019). Crank–Nicholson difference method and reproducing kernel function for third order fractional differential equations in the sense of Atangana–Baleanu Caputo derivative. *Chaos, Solitons and Fractals*, *127*, 10–16. https://doi.org/10.1016/j.chaos.2019.06.011

Aoife, L., & Jerry, D.M. (2019). Can green gas certificates allow for the accurate quantification of the energy supply and sustainability of biomethane from a range of sources for renewable heat and or transport?. *Renewable and Sustainable Energy Reviews*, *115*, 109347. https://doi.org/10.1016/j.rser.2019.109347

Basuki, I., Cari, & Suparmi. (2017). Visualization of heat transfer in material for varians of boundary value with Relaxation Iteration Gauss-Seidel method. *Journal of Physics: Conf. Series*, *795*, 012017. https://doi.org/10.1088/1742-6596/795/1/012017

Berezansky, L., & and Braverman, E. (2020). Solution estimates and stability tests for linear neutral differential Equations. *Applied Mathematics Letters*, *108*, 106515. https://doi.org/10.1016/j.aml.2020.106515

Boland, J. (2002). The analytic solution of the differential equations describing heat flow in houses. *Building and Environment*, *37*, 1027–1035. https://doi.org/10.1016/S0360-1323(01)00098-1

Brun, J.L., & Pacheco, A.F. (2005). Reducing The Heat Transfer Through a Wall. *Eur. J. Physics*, *26*, 11-18. https://doi.org/10.1088/0143-0807/26/1/002

Conte, D. (2020). Dynamical low-rank approximation to the solution of parabolic differential equations. *Applied Numerical Mathematics*, *156*, 377–384. https://doi.org/10.1016/j.apnum.2020.05.011

Da Silva, R., Prado, S.D., & Fernandes H.A. (2017). A new look on the stabilization of inverted pendulum with parametric excitation and large random frequencies: Analytical and numerical approaches. *Commun Nonlinear Sci*

Numer Simulat., 51, 105–114.https://doi.org/10.1016/j.cnsns.2017.04.002

Defraeye, T., Blockenc, B., & Carmeliet, J. (2013). Influence of uncertainty in heat–moisture transport properties on convective drying of porous materials by numerical modelling. *Chemical Engineering Research and Design*, *91*, 36–42.https://doi.org/10.1016/j.cherd.2012.06.011

Dogu, Y., & Aksit, M.F. (2006). Brush Seal Temperature Distribution Analysis. *J. Eng. Gas Turbines Power*, *128*, 599-609. https://doi.org/10.1115/1.2135817

Farahani, S., Yerra, V.A., & Pilla, S. (2020). Analysis of a hybrid process for manufacturing sheet metal-polymer structures using a conceptual tool design and an analytical-numerical Modeling. *Journal of Materials Processing Tech.*, *279*, 116533.https://doi.org/10.1016/j.jmatprotec.2019.116533

Gao, R. (2016). Milne method for solving uncertain differential equations. *Applied Mathematics and Computation*, *274*, 774–785. https://doi.org/10.1016/j.amc.2015.11.043

Gregori, D., Scazzosi, R., Nunes, S.G., Amico, S.C., Giglio, M., & Manes, A. (2020). Analytical and numerical modelling of high-velocity impact on multilayer alumina/aramid fiber composite ballistic shields: Improvement in modelling approaches. *Composites Part B*, *187*, 107830.https://doi.org/10.1016/j.compositesb.2020.107830

Hammer, Th. (2014). Atmospheric Pressure Plasma Application for Pollution Control in Industrial Processes. *Contrib. Plasma Phys.*, *54*, 187–201. https://doi.org/10.1002/ctpp.201310063

He, T., & Wang, T. (2019). A three-field smoothed formulation for partitioned fluid–structure interaction via nonlinear block-Gauss–Seidel procedure. *Numerical Heat Transfer, Part B: Fundamentals, 75*, 198-216. https://doi.org/10.1080/10407790.2019.1615786

Idesman, A., & Dey, B. (2020). New 25-point stencils with optimal accuracy for 2-D heat transfer problems. Comparison with the quadratic isogeometric elements. *Journal of Computational Physics, 418,* 109640. https://doi.org/10.1016/j.jcp.2020.109640

Karami, R., & Kamkari, B. (2020). Experimental investigation of the effect of perforated fins on thermal performance enhancement of vertical shell and tube latent heat energy storage systems. *Energy Conversion and Management*, *210,* 112679. https://doi.org/10.1016/j.enconman.2020.112679

Klametsdal Ø.S., Rasmussen, A.F., Meyner, O., & Lie K.A. (2020). Efficient reordered nonlinear Gauss–Seidel solvers with higher order for black-oil models", *Comput Geosc.*, *24*, 593-607. http://dx.doi.org/10.1007/s10596-019-09844-5

Liu, Z., Wang, G., & Yi, J. (2020). Study on heat transfer behaviors between Al-Mg-Si alloy and die material at different contactconditions based on inverse heat conduction algorithm. *Journal of Materials Research and Technology*, *9*, 1918-1928.

Luijendijk, E. (2019). Beo v1.0: Numerical model of heat flow and low-temperature thermochronology in hydrothermal systems. *Geosci. Model Dev.*, *12*, 4061–4073.https://doi.org/10.5194/gmd-12-4061-2019

Lu, K., Xu, H., He, H., Gao, S., Li, X., Zheng, C. Cheng, Y. (2020). Modulating Reactivity and Stability of Metallic Lithium via Atomic Doping", *J. Mater. Chem.* A, *2020*, 10363-10369. https://doi.org/10.1039/D0TA02176H

Michael, S., & Alexandre, D. (2020). The effect of heating rate, particle size and gas flow on the yield of charcoal during the pyrolysis of radiata pine wood", *Renewable Energy*, *151*, 419-425.

https://doi.org/10.1016/j.renene.2019.11.036

Mortazavi, M., & Moghaddam, S. (2016). Laplace transform solution of conjugate heat and mass transfer in falling film absorption process", *International Journal of Refrigeration*, *66*, 93-104. **Error! Hyperlink reference not valid.**

Motlagh, M.B., & Kalteh, M. (2020). Simulating the convective heat transfer of nanofluid Poiseuille flow in a nanochannel by molecular dynamics method', *International Communications in Heat and Mass Transfer*, *111*, 104478. https://doi.org/10.1016/j.icheatmasstransfer.2020.104478

Paradezhenko, G.V., Melnikov, N.B., & Reser, B.I. (2020). Numerical Continuation Method for Nonlinear System of Scalar and Functional Equation", *Computational Mathematics and Mathematical Physics*, *60*, 404-410.

Pu, B., & Yuan, X. (2019). The alternate iterative Gauss-Seidel Method for linear systems", *Journal of Physics: Conference Series*, *1411*, 012008.

Shen, Z., & Zhou, H. (2020). Predicting effective thermal and elastic properties of cementitious composites containing polydispersed hollow and core-shell micro-particles. *Cement and Concrete Composites*, *105*, 103439.https://doi.org/10.1016/j.cemconcomp.2019.103439

Stanley, C.M. (2019). Specific Heat at Constant Pressure from First Principles: Contributions from Fully Anharmonic Vibrations. *Mater. Res. Express*, *6*, 125924.

Tianbai, X., Kun, X., Qingdong, C., & Tiezheng, Q. (2018). An investigation of non-equilibrium heat transport in a gas system under external force field. *International Journal of Heat and Mass Transfer*, *126*, 362–379. https://doi.org/10.1016/j.ijheatmasstransfer.2018.05.035

Wu, P., Wang, Z., Li, X., Xu, Z., Yang, Y., & Yang, Q. (2020). Energy-saving analysis of air source heat pump integrated with a water storage tank for heating applications. *Building and Environment*, *180*, 107029.https://doi.org/10.1016/j.buildenv.2020.107029

Wu, S.L., Zhou, T., & Chen, X. (2020). A Gauss—Seidel Type Method for Dynamic Nonlinear Complementarity Problems. *SIAM J. Control Optim.*, *58*, 3389-3412. https://doi.org/10.1137/19M1268884

www.EnggineeringToolBox.com (1), Thermal Conductivity of common Materials and Gases. https://www.engineeringtoolbox.com/thermal-conductivity-d_429.html (25 April 2020)

www.EnggineeringToolBox.com (2), Thermal Conductivity of Metals, Metallic Elements and Alloys. https://www.engineeringtoolbox.com/thermal-conductivity-metals-d_858.html (25 April 2020)

www.EnggineeringToolBox.com (3) Densities of Solids. https://www.engineeringtoolbox.com/density-solids-d_1265.html (25 April 2020)

Vitanov, P., Harizanova, A., Ivanova, T., & Dikov, H. (2014). Low-temperature deposition of ultrathin SiO_2 films on Si substrates. *J. Phys.: Conf. Ser.*, 514, 012010. https://doi.org/10.1088/1742-6596/514/1/012010

Zhang, C., Chang, J., Liu, M., Feng, S., Shi, W., & Bao, W. (2017). Effect of heat release on movement characteristics of shock train in an Isolator. *Acta Astronautica*, *133*, 185–194. https://doi.org/10.1016/j.actaastro.2017.01.031

Zhang, Y., Gao, J., & Huang, Z. (2017). Hamming method for solving uncertain differential equations. *Applied Mathematics and Computation*, *313*, 331–341. https://doi.org/10.1016/j.amc.2017.05.080